University of Baghdad
College of Engineering
JOURNAL OF ENGINEERING

Journal of Engineering
journal homepage: www.joe.uobaghdad.edu.iq
Number 3 Volume 26 March 2020

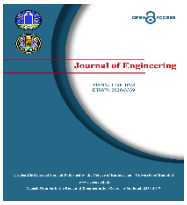

Civil and Architectural Engineering

Three-Dimensional Explicit Finite Element Simulation of Piled-Raft Foundation

Huda Hussein Ahmed *
M. Sc. Student
College of Engineering-University of Baghdad
Eng.huda81@gmail.com

Salah Rohaima Al-Zaidee
Assistant Professor
College of Engineering-University of Baghdad
salahalzaidee2004@gmail.com

ABSTRACT

This paper aims to validate a proposed finite element model to be adopted in predicting displacement and soil stresses of a piled-raft foundation. The proposed model adopts the solid element to simulate the raft, piles, and soil mass. An explicit integration scheme has been used to simulate nonlinear static aspects of the piled-raft foundation and to avoid the computational difficulties associated with the implicit finite element analysis.

The validation process is based on comparing the results of the proposed finite element model with those of a scaled-down experimental work achieved by other researchers. Centrifuge apparatus has been used in the experimental work to generate the required stresses to simulate the actual geostatic stress on the site. Comparing between numerical and experimental results indicate that the proposed finite element model is accurate and adequate and it can be used in future work to simulate more complicated practical problems of piled-raft foundations.

After its validation, this model was used to investigate the effectiveness of using piled with a raft foundation that subjected to eccentric loading. In this parametric study, the value of eccentricity e was taken equal to $B/12$, $B/6$, and $B/5$. The numerical results indicated that there is a significant decrease in the bearing capacity for unpiled raft foundation compared to the piled raft foundation for the same eccentricity of the applied load.

Keywords: Piled-raft Foundation, Mohr Coulomb Model, Explicit Dynamic, Finite Element Analysis.

المحاكاة الصريحة بالعناصر المحددة ثلاثية الابعاد لأسس الركائز الحصيرية

هدى حسين احمد *
طالب ماجستير
جامعة بغداد كلية الهندسة

صلاح رحيمة الزيدي
أستاذ مساعد
جامعة بغداد كلية الهندسة

لخلاصة

يهدف هذا البحث للتحقق من صحة نموذج العناصر المحددة المقترح اعتماده في تقدير الهطول وإجهادات التربة لأسس الركائز الحصيرية. يعتمد النموذج المقترح على العنصر الصلب لمحاكاة الأساس الحصيري والركيزة وكتلة التربة. تم استخدام مخطط

*Corresponding author
Peer review under the responsibility of University of Baghdad.
https://doi.org/10.31026/j.eng.2020.03.11

Article received:2/3/2019
Article accepted:57/5/2019
Article published:1/3/2020

التكامل الصريح لمحاكاة الجوانب الساكنة اللاخطية لأساسات الركائز الحصيرية وذلك لتجنب الصعوبات الحسابية المرتبطة بالتحليل الضمني بالعناصر المحددة.
تعتمد عملية التحقق من الصحة على مقارنة نتائج نموذج العناصر المحددة المقترح مع تلك الخاصة بالعمل التجريبي المصغر الذي تم اجراءه بواسطة باحثين آخرين. تم استخدام جهاز الطرد المركزي في العمل التجريبي لهؤلاء الباحثين لتوليد الضغوط المطلوبة لمحاكاة اجهاد التربة الفعلي في الموقع.
تشير المقارنة بين النتائج العددية والتجريبية إلى أن النموذج المقترح للعناصر المحددة دقيق وكاف ويمكن استخدامه في العمل المستقبلي لمحاكاة المشاكل العملية الأكثر تعقيدًا لأسس الركائز الحصيرية.
بعد التحقق من صحته، يمكن استخدام هذا النموذج في دراسة معيارية لفعالية استخدام الركائز مع مجموعة أسس حصيريه تعرض لأحمال لا مركزية. في هذه الدراسة المعيارية، يتم أخذ قيمة المسافة اللامركزية بقدار 12 / B و6 / B و5 / B
أشارت النتائج العددية إلى أن هناك انخفاض ملموس في قدرة التحمل للأساس الحصيري غير المستند على الركائز مقارنة بالأساس حصيري مستند على الركائز لنفس الحمل اللامركزي المطبق.
الكلمات الرئيسية: أسس الركائز الحصيرية، نموذج مور كولومب، الحركة الصريحة، التحليل بالعناصر المحددة.

1. INTRODUCTION

Piles have been used with the raft foundation for two primary reasons: first, to provide enough bearing capacity and second to decrease the settlements to an acceptable degree. The decreasing of settlement by piles means reduce the total settlement, for rigid foundations and decrease both the total and the differential settlements, for flexible foundations. **(Giretti, et al., 2009)**.

Physical, numerical, and analytical modeling approaches were used to investigate the performance of piled-raft foundations. The "Poulos Davis Randolph" (PDR) technique combines the analytical approaches proposed by **(Poulos and Davis, 1980)** and **(Randolph, 1994)** to analyze the piled raft foundations. **(Clancy and Randolph, 1993)** offered a "plate on spring" methodology in which the raft and the piles are performed as a plate and springs, respectively. **(Salman and Hamoudi,2015)** presented an analytical approach adopted on field data that had been used to calculate the strength capacity, deformations, and settlement for large diameter bored piles type with vertical and lateral load. Results indicated that there is an acceptable agreement of 12% between the field and analytical data. Numerical methods that are based on three-dimensional finite element modeling were proposed by **(Katzenbach et al.,1998)** and **(Sinha and Hanna, 2016)** presented a three-dimensional finite element model to simulate piled raft foundation. That study includes different parameters such as spacing, length, shape, and pile diameter. **(Emani and Raju, 2019)** presented a numerical analysis to simulate pile foundation and structure under seismic load. The behavior of piled-raft foundation was also investigated by using a centrifuge physical modeling **(Horikoshi,** and **Randolph., 1996), (Fioravante** and **Giretti, 2010),** and **(Alnuiam, et al., 2013**). The scaled-down model had been investigated by **(Al-Jorany and Al-Qaisee, 2016**). They presented an experimental model to investigate the behavior of piles installed in loss soil subjected to load axially. The effects of the horizontal distance of excavation, depth of excavation and pile slenderness ratios are investigated. The results showed the pile head deflection, settlement and bending moments along pile increase with decreasing horizontal distance between excavation face and adjacent axially loaded pile of various depths of excavation and pile slenderness ratios. **(Albusoda** and **Alsaddi, 2017**) presented a series of vertical and battered piles model tests installed in sandy soil and subjected to lateral loads. Different parameters are investigated, such as the pile batter inclination angle, pile spacing (s/d) ratio, number of piles and pile group configuration. Results revealed that changing the pile's number with the group using various patterns will influence the ultimate lateral resistance of the pile group.

This study aims to validate a proposed finite element model using Abaqus software with an explicit integration scheme to be adopted in predicting displacement and soil stresses of a piled-raft foundation.

2. EXPERIMENTAL WORK

The experimental work **(Fioravante** and **Giretti, 2010)** has been considered to validate and to discuss the results of the finite element model. This experimental work consists of four cases of square raft foundations that are supported on a soil mass only, a soil mass with single pile, a soil mass with the four piles, and a soil mass with nine piles, **Fig. 1**. The soil mass has been bounded by a container of $400mm$ in diameter and $492mm$ in depth. In the centrifuge system, a model is scaled down 65 times for the prototype material and for accelerated Earth's gravity to reproduce the same stress and strain in the model as in the prototype. Experiments have been achieved using dry sand with the finer grains of 15%, characterized by a maximum dry density, $\gamma_{d_{max}}$ of 16.50 kN/m^3, minimum dry density, $\gamma_{d_{min}}$of 13.08 kN/m^3, uniformity coefficient, C_U of 3.33, and the angle of shearing resistance, φ equals 35°.

A square steel plate raft model with dimensions of 115 mm wide; B, 25 mm thickness; t_r, and elastic modulus, E_r, of 2.1×10^5 MPa. The soil elastic modulus, E_s, of 115 MPa has been adopted. Poisson ratios, v_s, of 0.2 and 0.3 have been used for the soil and steel plate respectively. The closed-ended model of piles had a diameter, D, of 8 mm. and a length, L, of 292 mm. The test program consisted of five model schemes shown in **Fig. 2**.

At first, each soil model had been reconstituted to a relative density, D_R of, 60%. A very rigid frame, which held a hydraulic actuator, two linear displacement transducers (LDTs) to measure the raft displacement, a load cell to measure the vertical applied load, and the raft plate had been mounted onto the container top and then the model had been placed in the centrifuge and accelerated to 65g.

As the model was being submitted to the acceleration field in the centrifuge, the soil surface settled due to consolidation. The presented data refer to the average soil density achieved at the end of the in-flight consolidation, which was always about D_R of 70%, and it had been assumed constant with depth. At the end of the inflight consolidation, the model piles had been jacked completely with an approximate rate of about 2mm/s into the soil model at 65g.

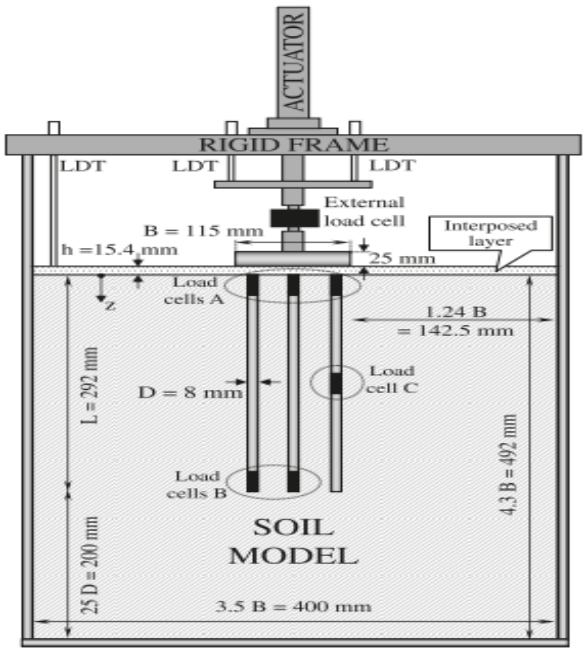

Figure 1. Test model and boundary conditions **(Fioravante** and **Giretti, 2010).**

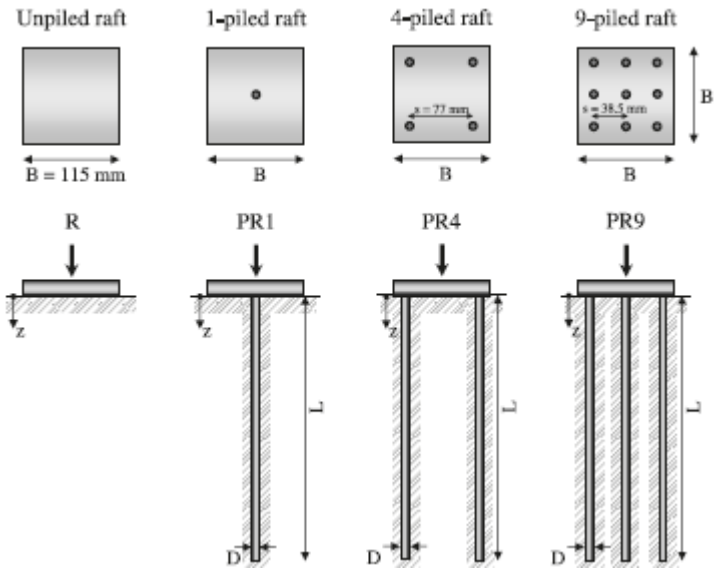

Figure 2. Model sketches. R, unpiled raft; PR1, raft with single pile; PR4, raft with four piles; PR9, raft with nine piles **(Fioravante** and **Giretti, 2010).**

3. FINITE ELEMENT MODEL

A three dimensional hexagonal and tetrahedral elements have been used to simulate the soil mass, pile, and the raft foundations, as indicated in **Fig. 3**. The tied constraint has been used to ensure the compatibility between the raft, the piles, and the soil mass. Radial roller and hinge supports have been used to model the stiffness of the container walls and base, respectively. Displacement controlled technique has been used to apply the pressure on the raft foundation in terms of the corresponding uniform displacement.

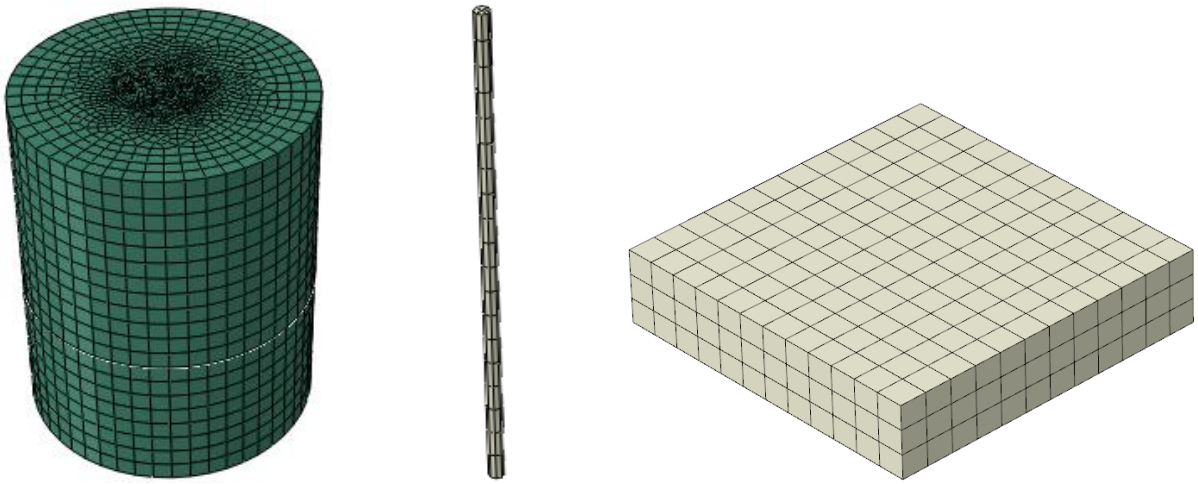

(a) Soil mass. **(b) Piles** **(c) Raft Foundation**

Figure 3 . Finite element mesh.

4. MOHR COULOMB MODEL

In this paper the plasticity model **(Chen, 1975)**, Mohr-Coulomb that is used to simulate granular materials under monotonic static loading with neglecting the loading rate have been adopted to model the sandy soil it is generally written as:

$$(\sigma_1 - \sigma_3) + (\sigma_1 + \sigma_3)\sin\varphi - 2c\cos\varphi = 0 \quad (1)$$

where $\sigma_1$and σ_3 are the maximum and minimum principal stresses (positive in tension), φ is the shearing angle., and c is the cohesion. Experimental works indicated that the intermediate principal stress, σ_2, has an insignificant effect on the yield of the model **(Menetrey** and **Willam, 1995)**. In the Abaqus environment, the following features have been adopted **(Chen, 1975)**.

- There is a region of purely linear elastic response, beyond which there would be a part of irrecoverable deformations that have to be simulated as plastic deformation.
- The material is assumed isotropic at the initial loading stage.
- The yielding behavior has been defined as a function of the hydrostatic pressure to have a stronger material for higher confining pressure.
- The isotropic model has been assumed for hardening or softening behavior.
- Hyperbolic and piecewise elliptic shapes have been respectively assumed for the smooth flow potential in the meridional stress plane and the deviatoric stress plane

The Mohr-Coulomb yield function takes the following shape:

$$F = R_{mc}q - p\tan\phi - c = 0 \quad (2)$$

where: $R_{mc}(\theta, \phi)$ is a function assigned to measure the shape for the yield surface in the deviatoric plane.

$$R_{mc} = \frac{1}{\sqrt{3}\cos\phi}\sin(\theta + \frac{\pi}{3}) + \frac{1}{3}\cos(\theta + \frac{\pi}{3})\tan\phi \quad (3)$$

ϕ is the slope of the Mohr-Coulomb yield surface in the stress plane $(q - p)$, as shown in **Fig. 4**, which is the angle of friction $0 \leq \phi \leq 90$, and θ is the deviatoric polar angle defined as:

$$\cos 3\theta = \frac{r^3}{q^3} \quad (4)$$

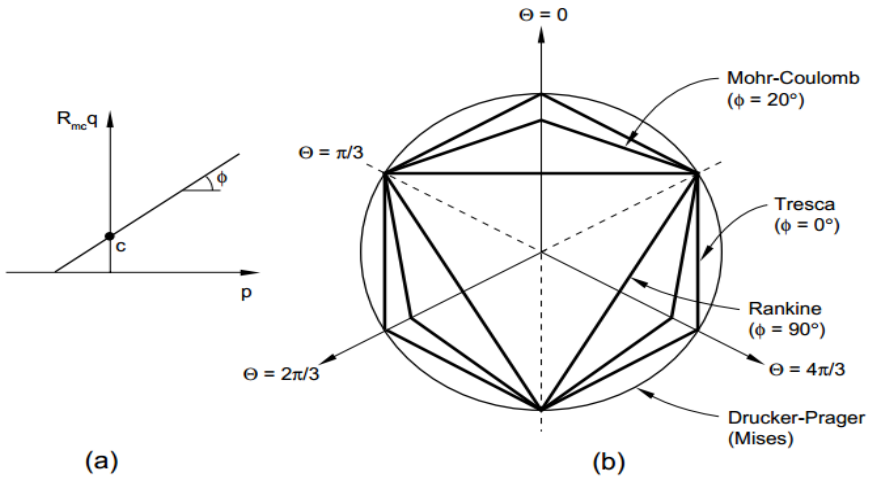

Figure 4. Yield surface in the meridional plane (a) and the deviatoric plane (b).

The flow potential has been chosen as a hyperbolic function in the meridional stress plane and the smooth elliptic function suggested by **(Menetrey** and **Willam, 1995)** in the deviatoric stress plane:

$$G = \sqrt{(\varepsilon c_0 \tan\psi)^2 + (R_{mw} q)^2} - p \tan\Psi \tag{5}$$

where G is the control for the shape in the meridional plane, c is the initial cohesion for material, Ψis the dilation angle, and ε is the meridional eccentricity as shown in **Fig. 5 (Menetrey** and **Willam, 1995)**.

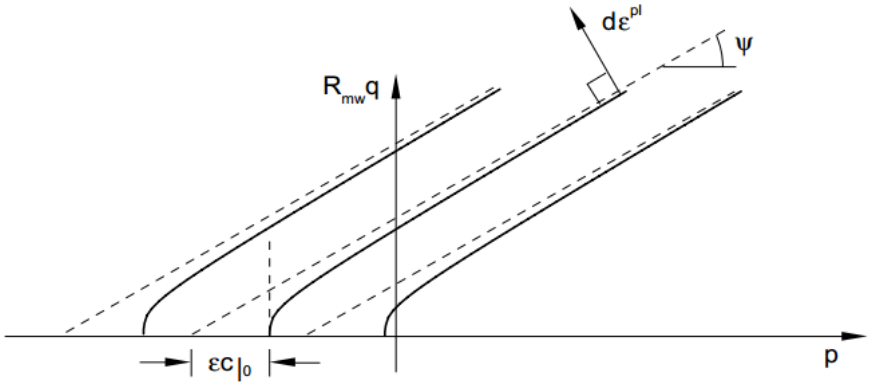

Figure 5 . Mohr-Coulomb flow potential in the meridional plane.

R_{mw} is the controls for the shape of G in the deviatoric plane:

$$\boldsymbol{R_{mw} = \frac{4(1-e^2)(\cos\theta)^2 + (2e-)^2}{2(1-e^2)\cos\theta + (2e-1)\sqrt{(4(1-e^2)(\cos\theta)^2 + 5e^2 - 4e)}} R_{mc}(\frac{\pi}{3}, \varphi)} \tag{6}$$

where

$$\boldsymbol{e = \frac{3 - \sin\varphi}{3 + \sin\varphi}} \tag{7}$$

5. EXPLICIT DYNAMICS ANALYSIS

To avoid the difficulties commonly associated with using the implicit integration scheme in finite element analysis of piled raft foundations that have large deformation, it is recommended to implement the explicit finite element integration scheme. The explicit step by step scheme is used to integrate the equations of motion through time in problems such as high-speed (short duration) dynamics, large nonlinear deformation, and quasi-static analyses. It is also known as the forward Euler or central difference, and it is based upon using the diagonal "lumped" element mass matrices. With this scheme, the displacement and velocity would be determined based on the following explicit central-difference integration rule **(Oden** and **KiKuchi, 1980)**.

$$\dot{u}^N_{(i+\frac{1}{2})} = \dot{u}^N_{(i-\frac{1}{2})} + \frac{\Delta t_{(i+1)} + \Delta t_{(i)}}{2} \ddot{u}^N_{(i)} \tag{8}$$

$$u^N_{(i+1)} = u^N_{(i)} + \Delta t_{(i+1)} \dot{u}^N_{(i+\frac{1}{2})} \tag{9}$$

where u^N is the degree of freedom, displacement or rotation. In this paper, u^N defines the nodal displacement for the solid element. i indicates the increment number in the step of explicit dynamics.

The central-difference integration is called explicit as the kinematic state that in advanced adopting identified values of $\dot{u}^N_{\left(i-\frac{1}{2}\right)}$ and $u^N_{(i)}$ from the previous increment **(Zienkiewice** and **Naylor, 1972)**. The explicit integration scheme is relatively simple, but it does not offer the computational efficiency required for the explicit dynamic procedure. Using the diagonal element mass matrices is the key to the computational efficiency of the explicit procedure because the accelerations of the increment are computed by:

$$\ddot{u}^N_{(i)} = (M^{NJ})^{-1}(P^J_{(i)} - I^J_{(i)}) \tag{10}$$

where M^{NJ} is the mass matrix, P^J and I^J are vectors for the applied load and the internal force, respectively. As it is simple to be inverted, a lumped mass matrix has been used. No iterations and no tangent stiffness matrix are required for the explicit procedure. The internal force vector, I^J , is assembled from contributions of the individual elements in such a way that no global stiffness matrix is needed **(Zienkiewice** and **Naylor, 1972)**. A nonzero nodal mass exists for all nodes of solid elements were used in this paper unless all activated translational degrees of freedom are constrained similarly to the case of the hinge support assigned to the base of the simulated soil mass. Regarding the nodes of the raft foundation rigid body, they do not require mass, but the entire rigid body raft must possess mass and inertia **(Abaqus Analysis User's Manual Volume II, 2009)**.

In the explicit procedure, integration is achieved through a time-domain using many small increments. The central difference operator is conditionally stable in accordance with following limit, which can be written in terms of the highest frequency of the system as:

$$\Delta t = \frac{2}{\omega_{maximum}} \tag{11}$$

Due to the computational difficulties associated with the determination of ω_{max} an approximation to the stability limit is usually determined based on the shortest transit time of a dilatational across a wave of the elements in the mesh.

$$\Delta t \approx \frac{L_{min}}{c_d} \tag{12}$$

where L_{min} is the least element dimension in the mesh and c_d is the dilatational wave speed that defines in terms of λ and μ. It should be mentioned that the estimated Δt is approximated in nature, and it is not conservative in most cases **(Oden** and **KiKuchi, 1980)**.
In Abaqus/Explicit, the actual stable time increment is selected to be less than the aforementioned estimated by a factor from $1/\sqrt{3}$ to 1 for three-dimensional models such as solid element model adopted in this paper **(Abaqus Analysis User's Manual Volume II, 2009)**. The current dilatational wave speed, c_d, is determined based on the following relation:

$$c_d = \sqrt{\frac{\lambda + 2\mu}{\rho}} \tag{13}$$

where λ is the effective Lamé's constants, ρ mass density, and μ is the shear modulus. For an isotropic, elastic material the effective Lamé's constant and shear modulus can be defined in terms of Young's modulus, E, and Poisson's ratio, ν by the following relations:

$$\lambda = \lambda_o = \frac{E\nu}{(1+\nu)(1-2\nu)} \tag{14}$$

$$\mu = \mu_o = \frac{E}{2(1+\nu)} \tag{15}$$

In Abaqus/Explicit the constants $\lambda \, and \, \mu$ are determined as follows. Define the increments , ΔS, Δe, and $\Delta \varepsilon_{vol}$ for the mean stress, the deviatoric stress, the deviatoric strain, and volumetric strain, respectively. Assuming a hypo-elastic stress-strain rule of the form:

$$\Delta p = (3\lambda + 2\mu)\Delta\varepsilon_{vol} \tag{16}$$

$$\Delta S = 2\mu\Delta e \tag{17}$$

The effective moduli can then be computed as:

$$3K = 3\lambda + 2\mu = \frac{\Delta p}{\Delta\varepsilon_{vol}} \tag{18}$$

$$2\mu = \frac{\Delta S : \Delta e}{\Delta e : \Delta e} \tag{19}$$

$$\lambda + 2\mu = \frac{1}{3}(3K + 4\mu) \tag{20}$$

The time increment adopted in an analysis has to be smaller than the indicated stability limit of the central-difference operator. Failure in using adequately small increments will lead to an

unstable solution. For the unstable solution, the time history response for solution variables will fluctuate with increasing amplitudes. The total energy balance will dramatically change. For a model with one material type, the initial time increment would be positively proportional to the size of the smallest element in the mesh. For a mesh with uniform size but contains multiple material descriptions, as in the case of this paper, the element with the maximum wave speed will control the initial time increment **(Oden** and **KiKuchi, 1980)**.

In nonlinear problems with large deformations and/or nonlinear material response as in the problem of the piled-raft foundation, the maximum frequency for the model will continuously change for a continuously be changed in the stability limit **(Oden** and **KiKuchi, 1980)**. Abaqus/Explicit offers two strategies, namely fully automatic time incrementation and fixed time incrementation to control the time increment **(Abaqus Analysis User's Manual Volume II, 2009)**. Full automatic time incrementation has been used through the numerical simulation of this paper.

6. VALIDATION OF THE FINITE ELEMENT MODEL

a. Nonlinear Three-dimensional Numerical Analysis

As discussed previously, this paper aims to validate the finite element model presented in Section 3 based on the experimental work of **(Fioravante** and **Giretti, 2010)**. In the presented finite element simulation, the piles and the raft are simulated by using three–dimensional solid finite elements. Perfect contact between raft, piles, and soil has been assumed during body assemblage as indicated in **Fig. 6**. A square raft with dimensions of 115 mm wide, B and 25 mm thickness, t_r steel plate characterized by an elastic modulus of $E_r = 2.1 \times 10^5\ MPa$. The model of piles had a diameter, D, of $8\,mm$ and a length, L, of $292\,mm$. The soil mass has interior dimensions of $0.4\,m$ in diameter, and $0.5\,m$ height, dimensions for soil mass has been selected to ensure stress dissipation at far boundaries. As indicated in **Fig. 7**, hinge supports are adopted to restrain the isolated soil mass. The raft is assumed rigid, while the piles are simulated as elastic. Mohr-Coulomb model has been used to simulate the elastoplastic behavior of the soil mass. Linear and isotropic, the elastic response of the soil mass is assumed with an elastic modulus, E_s, of $115\,MPa$ and a Poisson ratio, ν, of 0.2. The soil strength parameters are $\varphi = 35^{\circ}$and $c = 1$ and dilation angle $\psi = 0$.

The loads must be applied very slowly when the explicit dynamic model is used, to avoid "exciting" the inertial aspect of the finite element model. In the beginning, gravity load is applied to the soil mass then the vertical point load is applied by using a downward-displacement at the mid-top surface of the raft with $u = 5mm$ for a duration of 10 seconds.

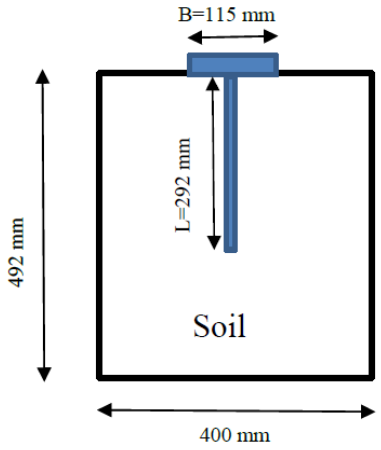

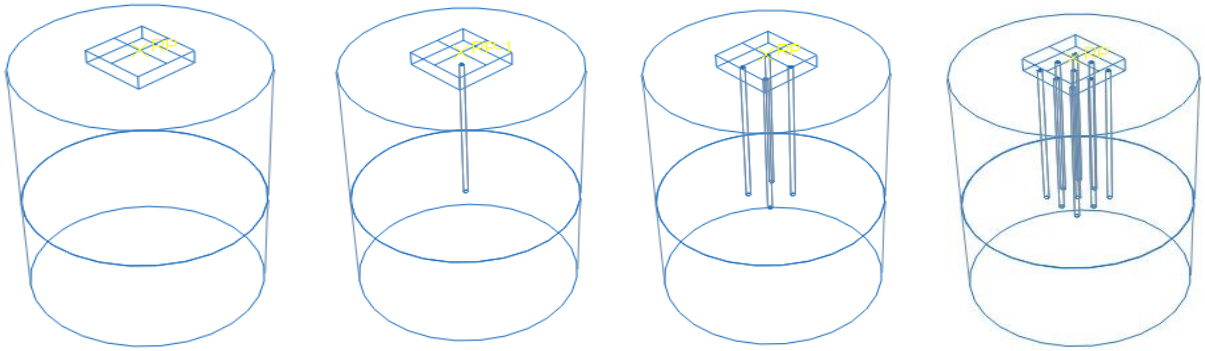

Figure 6. Raft and piled-raft foundation with soil mass.

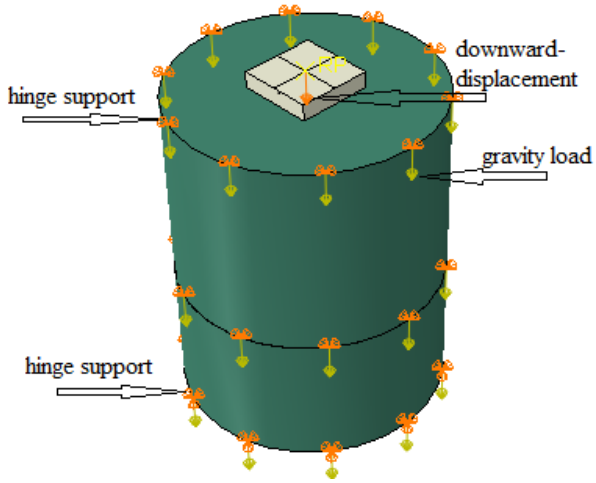

Figure 7. Boundary condition.

b. Results and Discussions

This section aims to presents the deformations, settlements, and stresses determined from the finite element analysis. Comparisons to the experimental results provided by **(Fioravante** and **Giretti, 2010)** were also included.

i.Raft Foundation

For the case of the raft foundation supported directly on the soil without piles, the displacements, and the stresses in soil mass are presented in **Fig. 8** and **Fig. 9**. **Fig. 10** indicates that the explicit dynamics finite element models give good agreement results with the experimental tests; therefore the proposed finite element model with explicit integration scheme seems valid and adequate to simulate the behavior of a raft foundation on sandy soil.

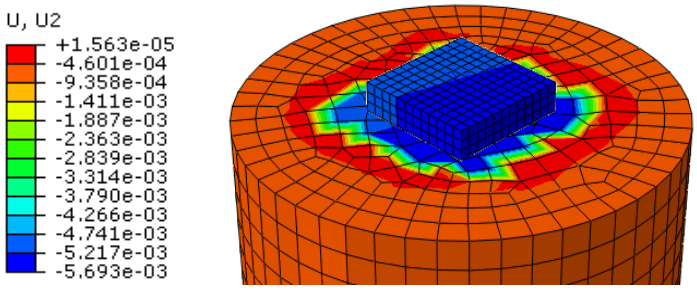

Figure 8. FE outcomes for displacement, (m), for the raft foundation (R).

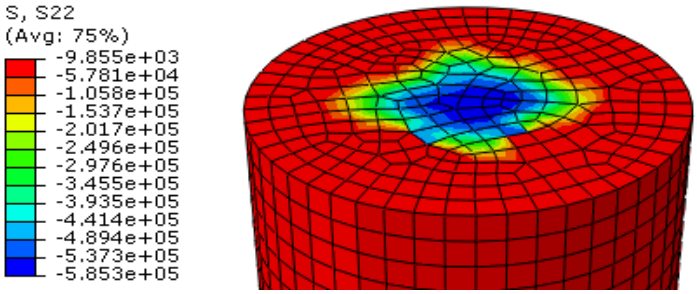

Figure 9. FE results for stresses in, (Pa), for the soil mass.

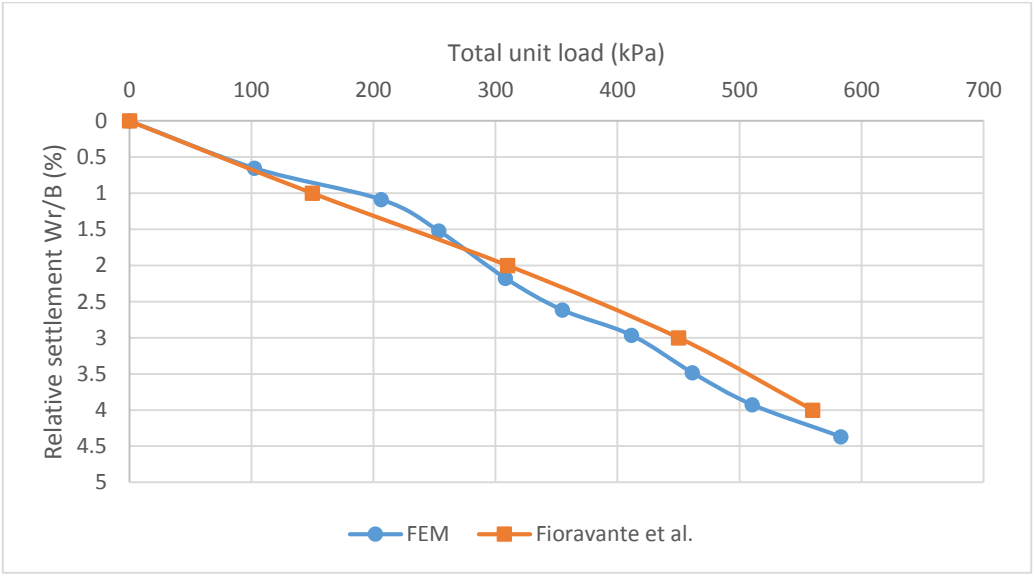

Figure 10. Load-displacement curves for the experimental work and finite element model for the raft foundation (R)

ii. Pile-raft Foundation

For piled-rafts supported on a single pile, four piles, and nine piles, displacements, soil stresses, and load-displacement curves have been presented in **Fig. 11** through **Fig. 19**. These figures indicate that the proposed finite element model is adequate to simulate the piled-raft foundations.

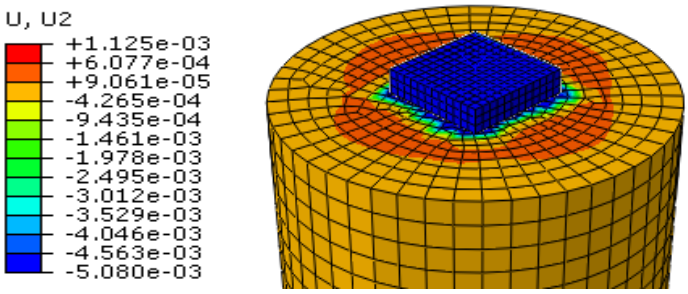

Figure 11. FE outcomes for displacement, (m), for the (PR1).

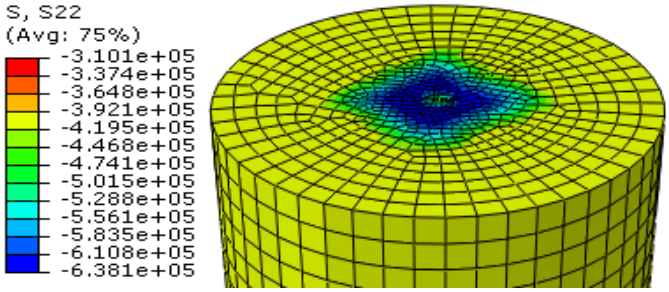

Figure 12. FE results for stresses in, (Pa), for the (PR1).

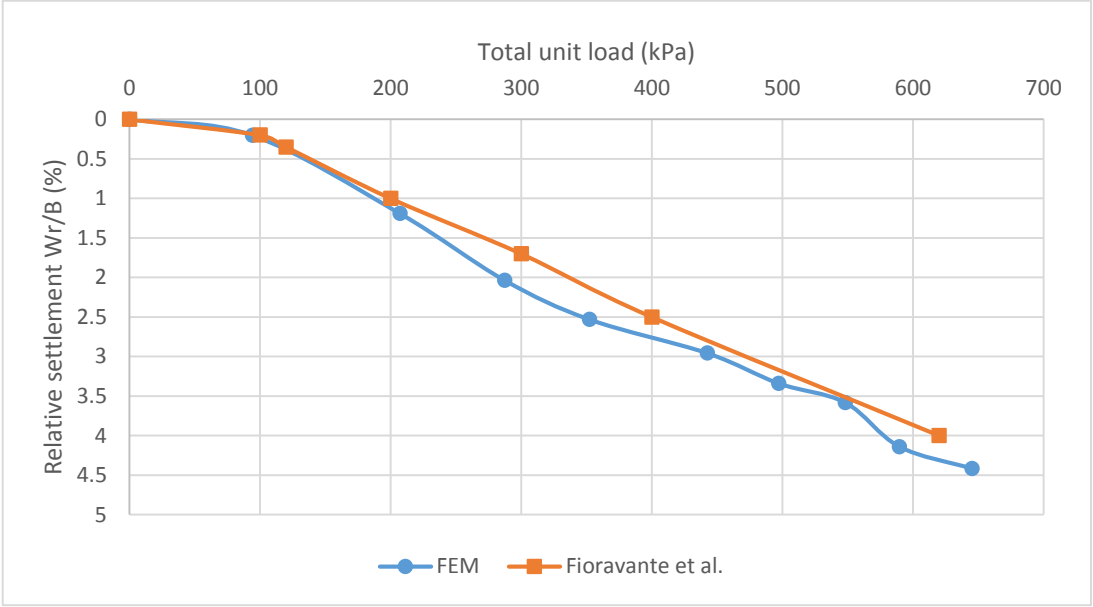

Figure 13. Load-displacement curves for the experimental work and finite element model for the (PR1).

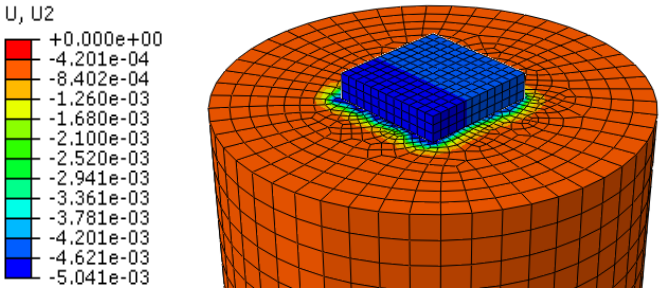

Figure 14. FE outcomes for displacement, (m), for the (PR4).

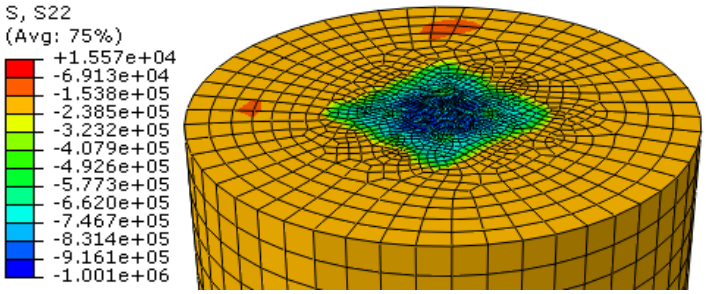

Figure 15. FE results for stresses in, (Pa), for the (PR4**).**

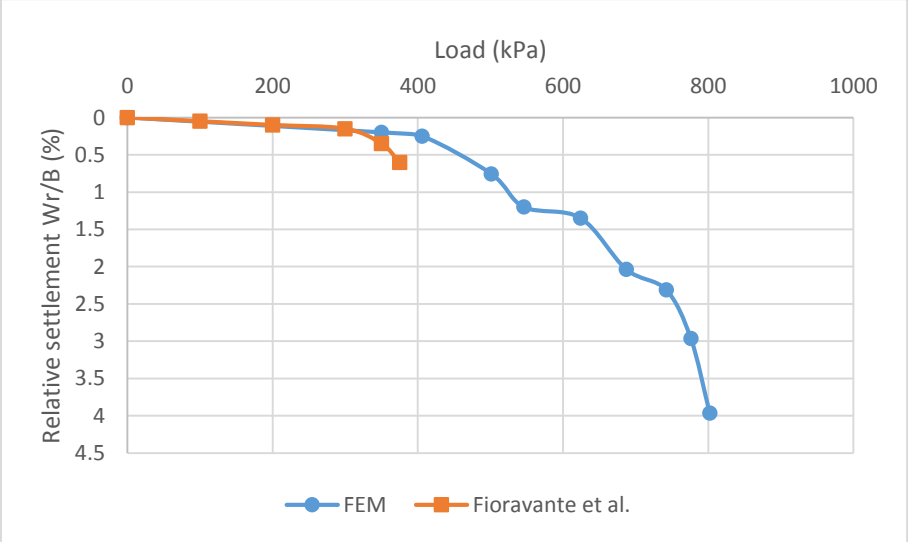

Figure 16. Load-displacement curves for the experimental work and finite element model for the (PR4).

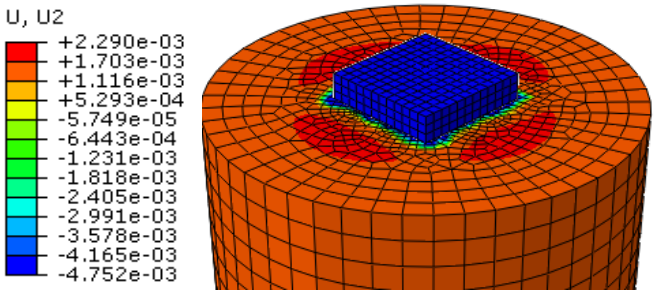

Figure 17. FE outcomes for displacement, (m), for the (PR9).

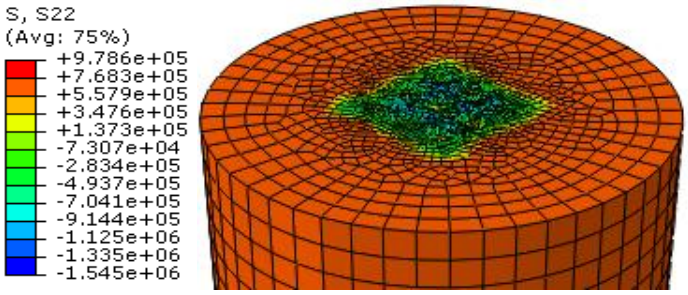

Figure 18. FE results for stresses in, (Pa), for the (PR9).

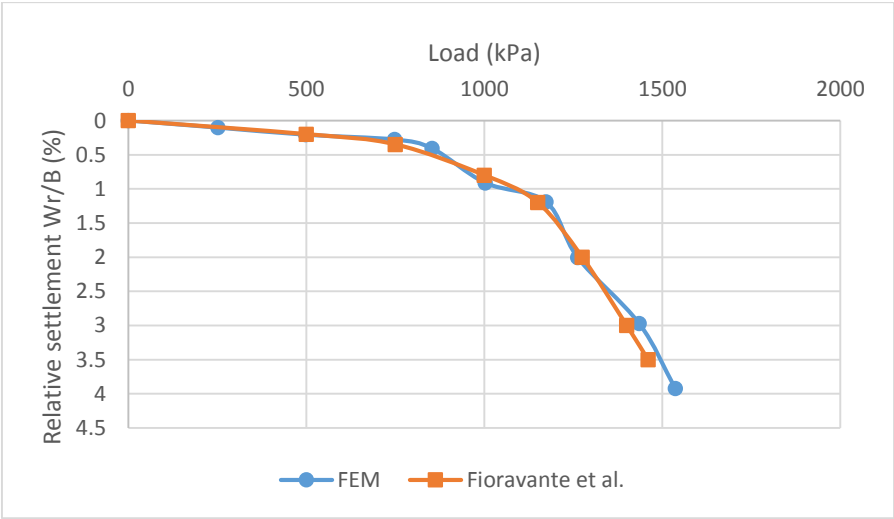

Figure 19. Load-displacement curves for the experimental work and finite element model for (PR9).

7. PARAMETRIC STUDY

After its validation, this model can be used for a parametric study. The primary objective of the parametric study is for the effectiveness of using piled with a raft foundation subjected to an

eccentric load. As shown in **Fig. 20** for the distance eccentricity, $e > B/6$, the pressure, q_{min} will be negative, which means that tension will develop. Because soil cannot take any tension, there will then be a separation between the foundation and the soil underneath it. In this parametric study, the value of e is taken $B/12$, $B/6$, and $B/5$.

A piled raft foundation with four piles has been adopted in this parametric study to evaluate the efficiency of an eccentric load. The piles used throughout this parametric study were 8 mm in diameter and 292 mm in length. The raft size was 115 mm wide and 25 mm thickness. The relative density for sandy soil was 60%.

A three dimensional hexagonal and tetrahedral elements have been used to simulate the soil mass, pile, and the raft foundations as discussed in Section 3. The nonlinear three-dimensional numerical analysis which is discussed in Section 6.1 has been adopted to simulate the models of the parametric study. Gravity load is applied to the soil mass then the vertical point load is applied by using a downward-displacement at the distance e in top surface of the raft with $u = 5mm$ for a duration of 10 seconds.

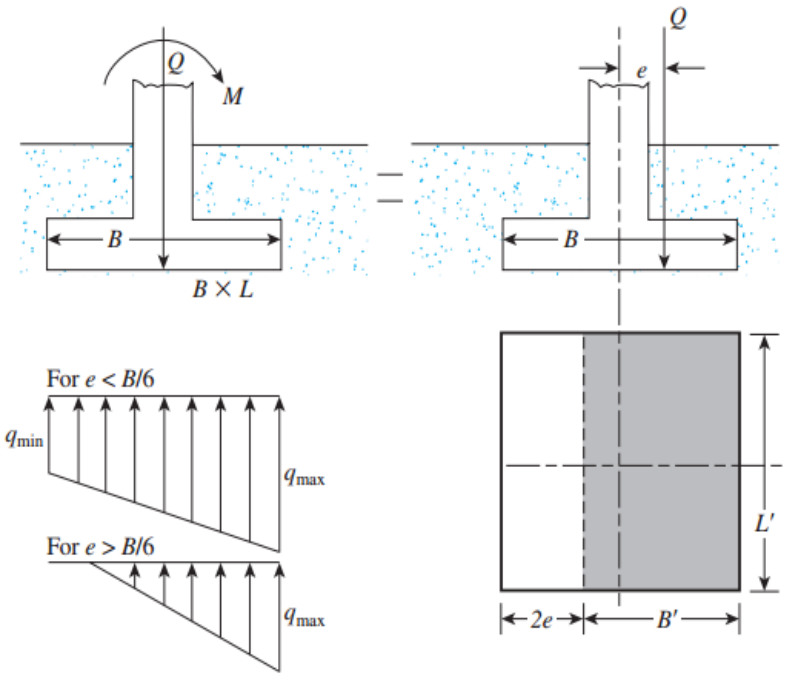

Figure 20. Eccentrically loaded foundations.

a. Results for the Effective of Load Eccentricity

The comparison between piled-raft foundations supported on four piles and unpiled raft foundations with different eccentricity load are presented through load-displacement curves indicated in **Fig. 21**. This figure indicates that the bearing pressures of unpiled rafts decrease significantly with an increase in the load eccentricity. Also, at same load level, greater displacements can be observed with increased load eccentricity. On the other hand, there is a significate decrease in bearing pressures for piled raft foundation comparing with unpiled raft foundation for the same eccentricity load and this decrease reduces as the eccentricity load increases. This parametric study indicates a reduction in bearing pressure about 39%, 33%, and 30% for piled raft foundations compared to unpiled raft foundations at eccentricity e of B/12, B/6, and B/5, respectively.

So using piles adjacent to the raft edges not only significantly increases the raft bearing pressures but also leads to a decrease in the raft displacement and tilts required to achieve the allowable limits of the raft settlements.

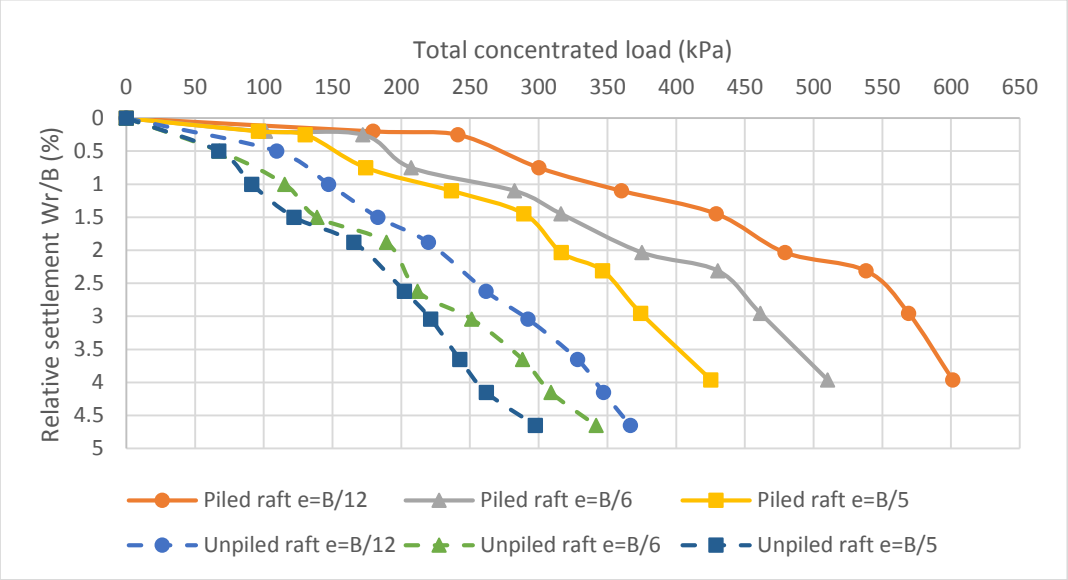

Figure 21. Load-displacement curve for piled raft and unpiled raft with different eccentricity loads.

8. CONCLUSIONS

Above figures for displacements, soil stresses, and the load-displacement curve indicate that the finite element model with the following features:

- A solid element for raft, soil, and pile.
- Mohr-Coulomb model for the elastoplastic behavior of soil mass.
- Explicit dynamic to simulate large displacement.

is adequate to simulate a raft foundation without piles and with a single pile, four piles, and nine piles. The accuracy and adequacy of the model have been assessed based on comparing its results with those obtained from the experimental work of **(Fioravante** and **Giretti, 2010)**.

After its validation, this model can be used for future research and design problems that relatively difficult to be analyzed based on experimental work and/or empirical relations.

Subsequently, the validated finite element model has been adopted in a parametric study considering a piled raft subjected to a point load with different eccentricities. The results indicate that there is a significant decrease in the bearing capacity for unpiled raft foundation compared to the piled raft foundation for the same eccentricity of the applied load. This parametric study indicates a reduction in bearing pressure about 39%, 33%, and 30% for piled raft foundations compared with unpiled raft foundations at eccentricity *e* of B/12, B/6, and B/5, respectively.

9. REFERENCES

- Abaqus Analysis User's Manual Volume II. 2009.
- Albusoda, N. S. and Alsaddi, A. F. 2017. *Experimental Study on Performance of Laterally loaded Plumb and Battered Piles in Layered Sand*. Journal of Engineering, pp. 23-37, Vol. 23, No. 9.
- Al-Jorany, A. N. and Al-Qaisee, G. S. 2016. *Experimental Investigating of Unsupported Excavation Considering Its Effect on a Nearby Axially Loaded Pile*. Journal of Engineering, pp. 17-31, Vol. 22, No. 6.
- Alnuiam, A., El Naggar, H., and El Naggar, M. H. 2013. *Performance of Piled-Raft System under* Axial Load. Proceedings of the 18th International Conference on Soil Mechanics and Geotechnical Engineering. 77, 91–105.
- Al-Saidi, A. A. 2016. *Correction Factor for Methods of Installation of piles Group in Sandy Iraqi Soils*. Journals of Engineering, pp. 172-181, Vol. 22, No. 9.
- Chen, W. F. 1975. *Limit Analysis and Soil Plasticity*. Amsterdam: Elsevier.
- Clancy, P., and Randolph, M. F. 1993. *An Approximate Analysis Procedure for Piled Raft foundations*. International Journal for Numerical and Analytical Methods in Geomechanics 17(12),849-869.
- Emani, P. K. and Raju, J. R. 2019. *Numerical Simulation of Seismic Interaction of Pile Foundation and Structure*. Geotechnical Earthquake Engineering, pp. 141-167.
- Fioravante, V., and Giretti, D. 2010. *Contact Versus Noncontact Piled Raft Foundations*. Can. Geotech. J. 47: 1271–1287 (2010): NRC Research Press.
- Giretti, D., Fioravante, V., & Jamiolkowski, M. 2009. *Modelling of Piled Raft Foundations In Sand*. Can. Geotech. J. 24: 1362–1376 (2009): NRC Research Press.
- Horikoshi, K. & Randolph, M. F., 1996. doi.10.1680/geot.1996.46.4.741. Centrifuge modelling of piled raft foundations on clay. Géotechnique, pp. 46(4):741-752
- Logan, D. L. 2007. *A First Course in the Finite Element Method, Fourth Edition*. s.l.: Nelson, a division of Thomson Canada Limited.
- Menetrey, P., and Willam, K. J. 1995. *Triaxial Failure Criterion for Concrete and its Generalization*. ACI Structural Jurnal, vol. 92, pp. 331-318.
- Oden, J. T., and KiKuchi, N. 1980. *Finite Element Methods for Constrained Problems in Elasticity*. Texas: TICOM. University of Texas at Austin.
- Poulos, H. G., and Davis 1980. *Piled Raft Foundations: Design and Applications*. Géotechnique, 51(2): 95-113.

- Randolph, M. F. 1994. *Design Methods for Piled Groups and Piled Rafts*. In Proceedings of the 13th international conference on soil mechanics and foundation engineering, Issue New Delhi, India, pp. 61-82.

- Salman, D. A., and Hamoudi, A., 2015. *Analytical Approach for Load Capacity of Large Diameter Bored Piles Using Field Data*. Journal of Engineering, pp. 40-54, Vol. 21, No 8.

- Sinha, A. and Hanna, A. 2016. 3D *Numerical Model for Piled Raft Foundation*. International Journal of Geomechanics, pp. 17(2), 04016055.

- Wang, G., and Sitar, N. 2004. *Numerical Analysis of Piles In Elasto-Plastic Soils Under Axial Loading*. 17th ASCE.

- Zienkiewice, O. C., and Naylor, D. J. 1972. *The Adaptation of Critical State Soil Mechanics Theory for Use in Finite Elements*. London.